

NASA-CR-202433

## INTERCHANGE # NCC2-5076

(22 July 1994 - 21 July 1996)

FINAL REPORT**The Martian Dust Cycle: Investigation of the Surface Lifting Component**

Dr. James R. Murphy, San Jose State University Foundation

Dr. Alison F.C. Bridger, Department of Meteorology, San Jose State University

Dr. Robert M. Haberle, Theoretical Studies Branch, NASA Ames Research Center

We have investigated the nature of the annual cycle of suspended dust in the martian atmosphere. This has been undertaken to understand the dynamical processes responsible for lifting dust from the surface, locations where dust is preferentially lifted, and preferred sites for dust deposition upon the surface. Our efforts have involved carrying out a number of numerical simulations with the Ames Mars General Circulation Model (GCM) interactively coupled with an aerosol transport/microrphysical model. The model generates an annual dust cycle similar to that observed. Various feedbacks are present in the atmosphere / surface system which enter into the generation of the cycle. Several locations are primary surface sources of dust, while much of the remaining planet's surface acts a sink for suspended dust.

## METHOD

Our efforts began by incorporating into our coupled model system a self consistent determination of the rate of surface dust lifting based upon the GCM calculated atmospher-surface momentum transfer (accounted for in the surface stress term). The relationship between surface stress and the flux of dust (mass per area per time) from the surface into the atmosphere is based upon empirically derived values under terrestrial conditions which have been used in terrestrial numerical modelling (Westphal et al., 1987). We explored the parameter space surrounding our prescription for the functionality of the lifting rate, as well as the threshold stress value ( $0.0225 \text{ N m}^{-2}$ ) below which no dust lifting occurs. (This threshold stress value chosen approximately corresponds to wind speeds of  $40 \text{ m s}^{-1}$  at the model grid-point nearest to the surface.) These sensitivity studies indicated that our choices were valid, with neither excessive nor minimal dust lifting being a constant product of the model. Rather, varying the initial conditions (with or without preexisting

suspended dust, with or without topography) resulted in a range of resulting quantities of lifted dust.

Having demonstrated the stability of the model, we proceeded to carry out a number of annual and multi-annual simulations. These simulations had as their initial condition the GCM state after running 1.25 years with a fixed dust load of optical depth 0.3 over the globe. Northern summer was chosen as the initial point since it has historically been the least dusty time of the year, and we desired the model to have developed its own self consistent state (to have become independent of the initial conditions) prior to entrance into the 'dust storm season', which begins in early northern autumn.

## RESULTS

Our nominal simulation, which extended through two martian years, produced an annual dust cycle similar to that inferred from observations. Two maxima of atmospheric dust loading occurred during northern autumn and winter (Figure 1). The first maximum, at  $L_S \sim 215$ , coincided in time with the first global dust storm observed by the Viking landers and orbiters during the first Viking year (July 1976 - May 1978). [ $L_S$  is a seasonal indicator for Mars:  $L_S=0$  corresponds to northern hemisphere (NH) spring equinox,  $L_S=90$  to NH summer solstice,  $L_S=180$  to NH autumn equinox, and  $L_S=270$  to NH winter solstice]. The primary model source region for the dust of this event was the northern and eastern slopes of the Tharsis uplands at northern subtropical latitudes, to the west of the Viking lander 1 site. Observations indicate that the first Viking year 1 dust storm had its genesis region at southern subtropical latitudes south and east of Tharsis. The second modelled maximum, at  $L_S \sim 270$ , coincided seasonally with the second, more intense global dust storm observed by Viking in 1977. This second modelled maximum had its primary dust source region on the northern slopes of the Hellas impact basin at southern subtropical latitudes. This topographic feature has been historically noted as a dusty locale, and in fact several global dust storms are thought to have originated there. The second 1977 dust storm was inferred from orbital imaging to have started in the same location as the first observed storm, south and east of Tharsis.

Following the second modelled atmospheric dust maximum, the atmospheric dust load declined to nearly zero by early northern spring ( $L_S=30$ ) (Figure 1). The modelled dust optical depth near the two lander site locations followed this same pattern (Figure 2). This retreat to a clear atmosphere is at odds with observations, which indicated during the Viking mission time period that during northern summer there was a 'background' optical depth of 0.2-0.4 at the Viking lander sites (Figure 3). Subsequent Earth-based observations have suggested that, at the present, the

aphelion season ( $\sim L_s=70$ ) might in fact be less dusty than was seen by Viking (Clancy et al., 1995)

Over the course of the simulated annual dust cycle, more dust was lifted in the northern hemisphere than in the southern hemisphere (Figure 4). This contrasts with the inferred hemispheric lifting distribution, since all the observed global storms have had a southern hemisphere origin. In the northern hemisphere, active dynamical processes involved in dust lifting include eastward travelling baroclinic waves (cold and warm frontal systems) at middle latitudes during autumn, winter, and spring. Additionally, winds down the north slope of Tharsis are a major source mechanism, especially during early autumn.

At equatorial latitudes, the most active source region was in the lowlands east of Tharsis. This location is the site of the cross-equatorial low level jet / western boundary current discussed by Joshi et al. [1995,1996] and was most active during the second lifting maximum as the Hadley cell accelerated due to the thermal drive provided by the suspended dust.

In the southern hemisphere, the predominant dust lifting sites were the northern and southern flanks of the Hellas basin. These sites were active only from late northern summer through late northern winter. Two additional sites, centred near 30S - 20W and 30S - 180W, were active source regions during the second lifting maximum only. These locations coincide with zones of enhanced low-level westerly jets resulting from the eastward Coriolis turning of the strong longitudinally confined cross-equatorial flow as discussed by Joshi et al. [1996]. At high southern latitudes, dust lifting extends poleward as the seasonal CO<sub>2</sub> cap retreats during southern spring, but this lifting is confined to the southern extent of Hellas and to longitudes extending only ninety degrees west from Hellas. Orbiter observations do indicate that the region near the retreating edge of the south seasonal polar cap does experience dust lifting, as the model suggests. The model also indicates a similar poleward expansion of northern hemisphere lifting in apparent conjunction with the retreat of the seasonal cap (Figure 5). Orbiter observations at this location and time are not suggestive of lifting then, the north cap generally shrouded by water ice clouds during this time period.

Continuation of this simulation through a second martian year resulted in a dust cycle for year two which differed very little from that of the first year.

To determine the nature of any feedbacks playing a role in producing the modelled dust cycle, a series of additional experiments was carried out. In one such experiment, the dust lifted into the atmosphere was radiatively inert (i.e., did not absorb solar radiation nor emit or absorb infrared radiation). In this case (Figure 6), substantial dust lifting commenced at the same season as in the nominal, radiatively active dust simulation. However, this inert dust simulation produced only a single dust lifting maximum, centered in time between the two maxima in the nominal experiment. The total quantity of dust lifted in this 'clear atmosphere' case actually exceeded that from the

nominal simulation by a factor of two. Most of the dust lifting occurred at northern middle latitudes during northern autumn, winter, and spring. The retreating cap edges played a more important role, in both hemispheres, in generating dust lifting than was the case in the nominal experiment. This is most likely due to the greater thermal contrast between the air above the cold ice covered ground and neighboring bare ground, this difference being reduced when radiatively active dust is present. This experiment, when compared to the nominal case, indicates that suspended dust during early northern autumn apparently has a negative feedback upon continued dust lifting into late autumn. The pattern of lifting indicates both positive and negative feedbacks on a local scale. Hellas lifting is greatly reduced for clear conditions, while northern middle latitude (baroclinic wave) lifting is enhanced.

Several other annual simulations indicate some dependence of the annual cycle upon the availability of liftable dust, but without having explicitly incorporated a finite amount of dust, and an initial spatial distribution, the results from these experiments are not quantitatively illuminating. One simulation indicates that the surface atmospheric density variation engendered by the atmospheric mass cycle, whereby twenty percent of the atmospheric ( $\text{CO}_2$ ) mass is condensed upon and subsequently sublimates from the seasonal polar ice caps, does not under present conditions play an important role in the current dust cycle. The horizontal mass flow to and from the condensing/sublimating caps may, however, be important.

The one major failing of our model was its inability to retain a background dust 'haze' during northern late spring and summer. We have attempted to account for this by including in the model an additional source mechanism: dust devils. Viking orbiter imaging and lander meteorology data indicate the presence on Mars of small (< 2 km diameter) vortices which contain moderate quantities of suspended dust. These were seen from orbit to be common occurrences on northern hemisphere plains during summer afternoons [Thomas and Gierasch, 1985]. The lander data indicated the occurrence of vortices during all seasons [Ryan and Lucich, 1983], but these features did not necessarily have suspended dust associated with them. Using the statistical occurrence of such features in orbiter imaging, and estimates of the dust contained within them, we have included a 'dust devil' dust lifting mechanism in our model which adds dust for only two hours per sol (1PM to 3PM) at those latitudes within 15 degrees of the subsolar latitude. Inclusion of this small additional, seasonally moving source produces optical depths at the model grid points corresponding to the Viking lander sites which compare very well with observed optical depth values during northern summer. Atmospheric temperatures also compare more favorably to middle atmospheric temperatures obtained from orbiter data.

## CONCLUSIONS

We have developed an atmospheric dynamical/aerosol model of the martian atmosphere which is capable, with only moderate tuning, of qualitatively and quantitatively reproducing the martian annual dust cycle as inferred from data obtained by the Viking orbiters/landers mission. Observed preferred dust source locations (Hellas basin, retreating cap edge) are preferred dust source locations in the model. The occurrence of two lifting maxima during northern autumn/winter arise due to a negative feedback between suspended dust during early northern autumn and the ability to sustain, or increase, the lifting rate into late autumn. It is only when the early autumn dust maximum has declined (to a global optical depth of  $\sim 0.8$ ) that lifting can increase again and produce the second maximum near the time of northern winter solstice. The seasonal cycle of CO<sub>2</sub>, as it affects surface pressure and thus surface density, is not an important factor in determining the present martian dust cycle.

A paper describing this work is in final preparation, and will be submitted to either the Journal of Geophysical Research or to the journal Icarus.

## REFERENCES

- Joshi, M. M., S.R. Lewis, P.L. Read, and D.C. Catling, 1995, Western boundary currents in the martian atmosphere: numerical simulations and observational evidence, *J. Geophys. Res.*, 100, 5485-5500.
- Joshi, M.M., R.M. Haberle, J.R. Barnes, J.R. Murphy, and J. Schaeffer, 1996, Low level jets in the NASA-Ames Mars GCM, submitted to *J. Geophys. Res.*, in revision.
- Ryan, J.A., and R.D. Lucich, 1983, Possible dust devils, vortices on Mars, *Journ. Geophys. Res.*, 88, 11005-11011.
- Thomas, P., and P.J. Gierasch, 1985, Dust devils on Mars, *Science*, 230, 175-177.
- Westphal, D.L., O.B. Toon, and T.N. Carlson, 1987, A two-dimensional numerical investigation of the dynamics and microphysics of Saharan dust storms, *Journ. Geophys. Res.*, 92, 3027-3049.

# GLOBAL DUST LIFTING PER SOL ( $\text{g m}^{-2}$ )

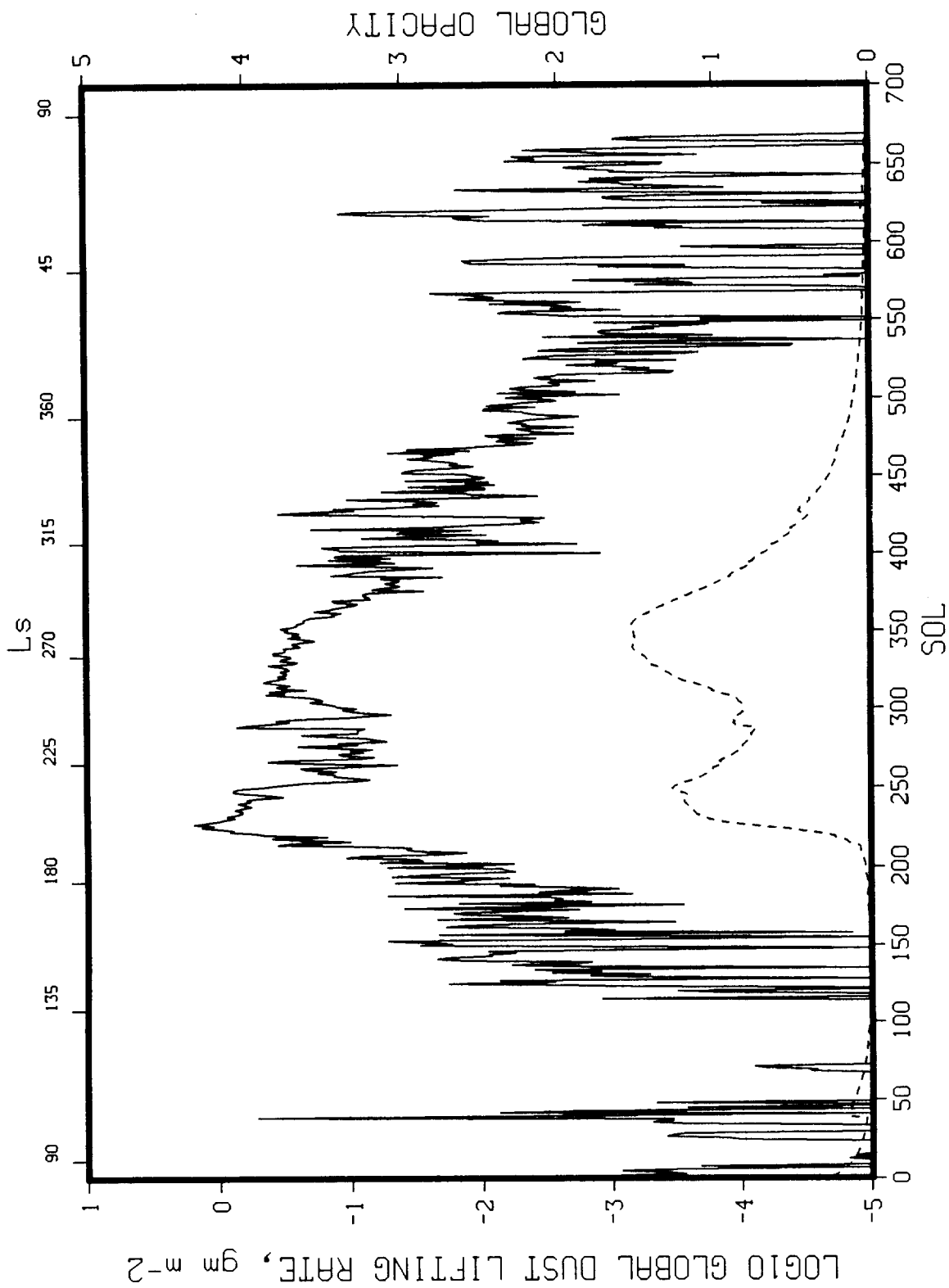


Figure 1. Time history of sol mean dust lifting rate (SOLID) and globally integrated dust optical depth (DASHED) during the course of the first year of the nominal simulation.

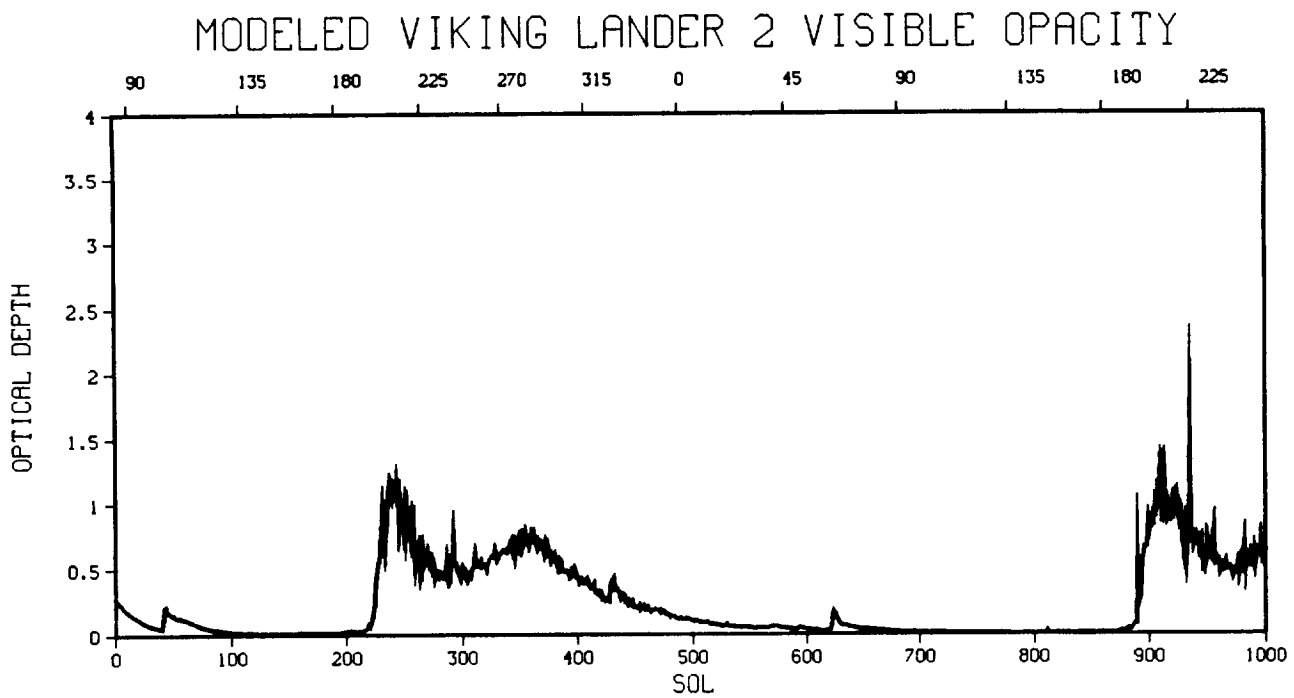
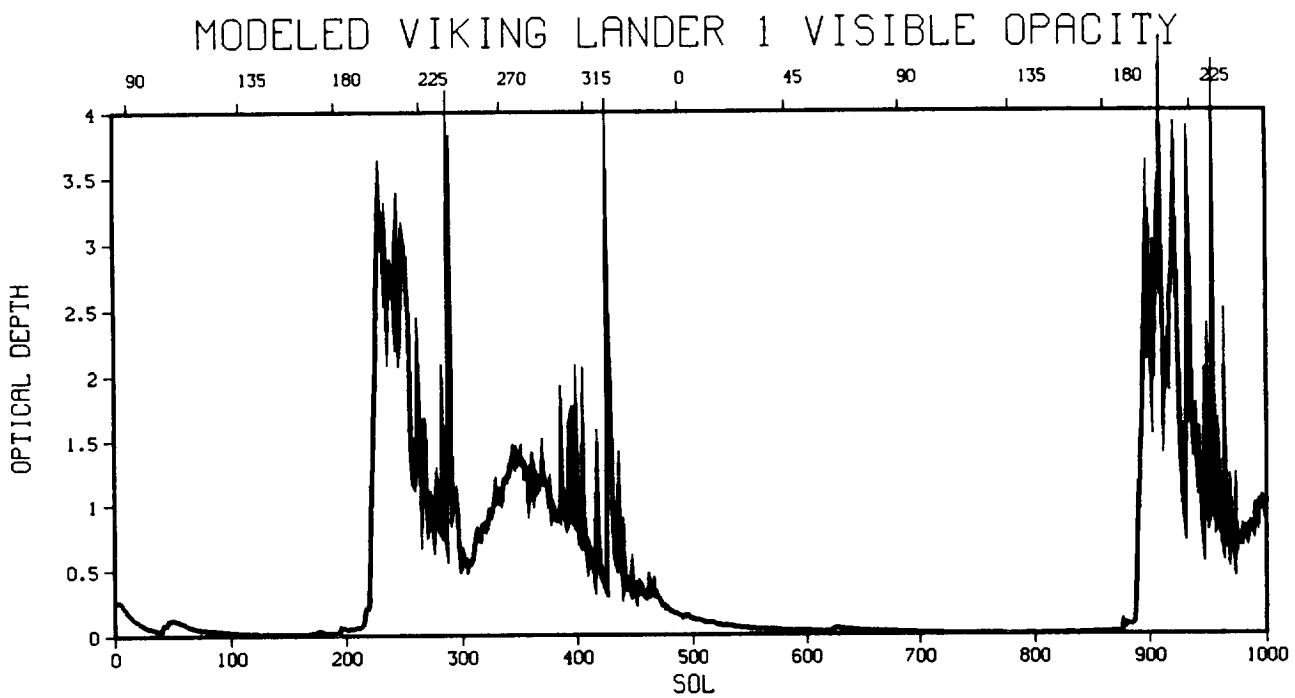


Figure 2. Time history of model generated visible dust optical depth at the equivalent Viking lander locations during the first 1.5 years of the nominal simulation.

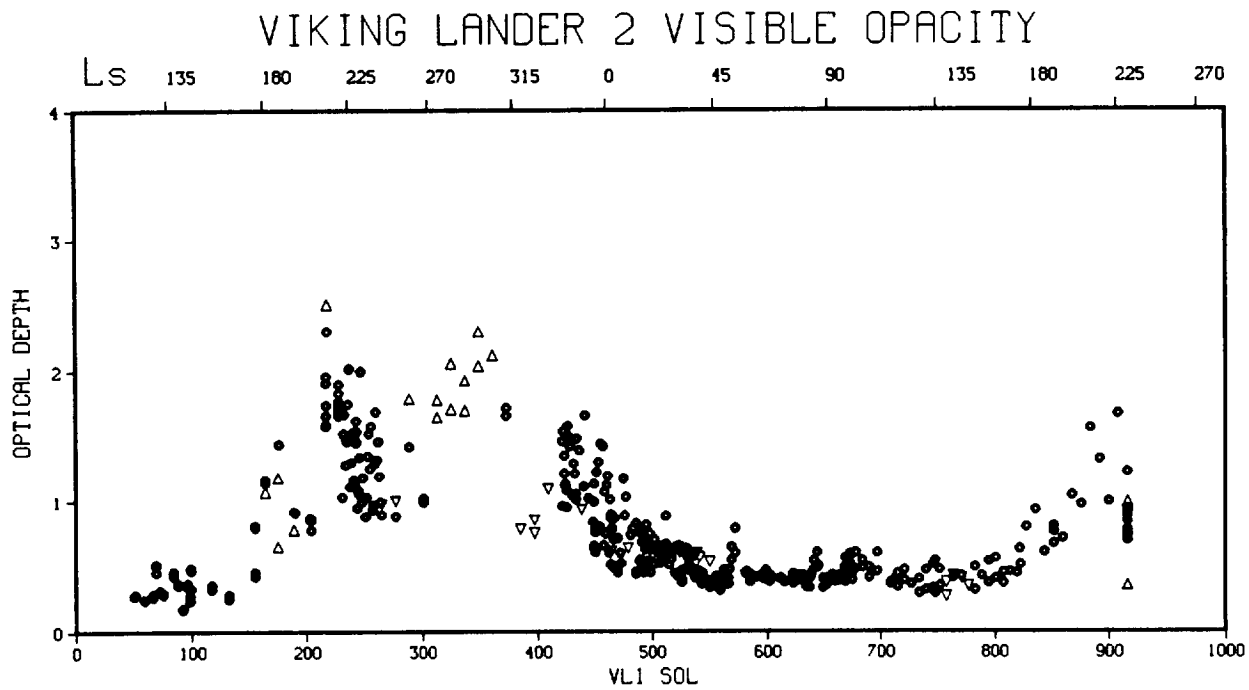
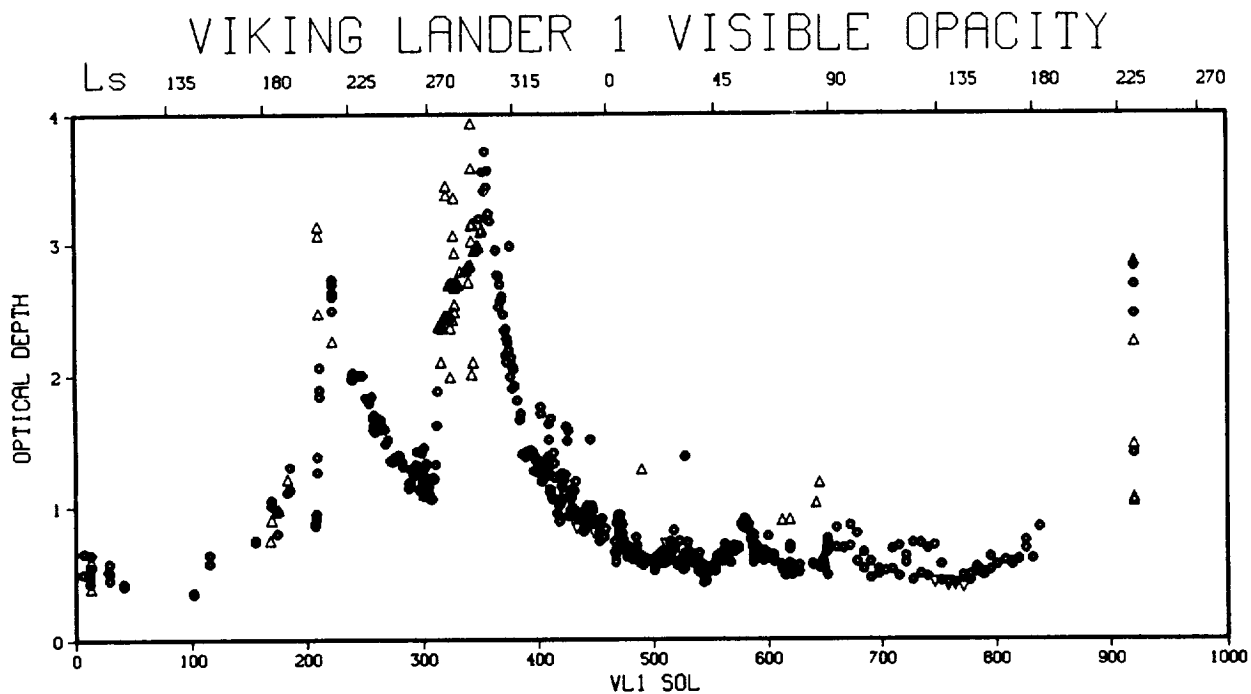


Figure 3. Time history of the observed visible optical depth at the the Viking lander sites during the initial 1.5 years of the mission.



TOTAL SURFACE DUST LIFTING, gm m<sup>-2</sup>

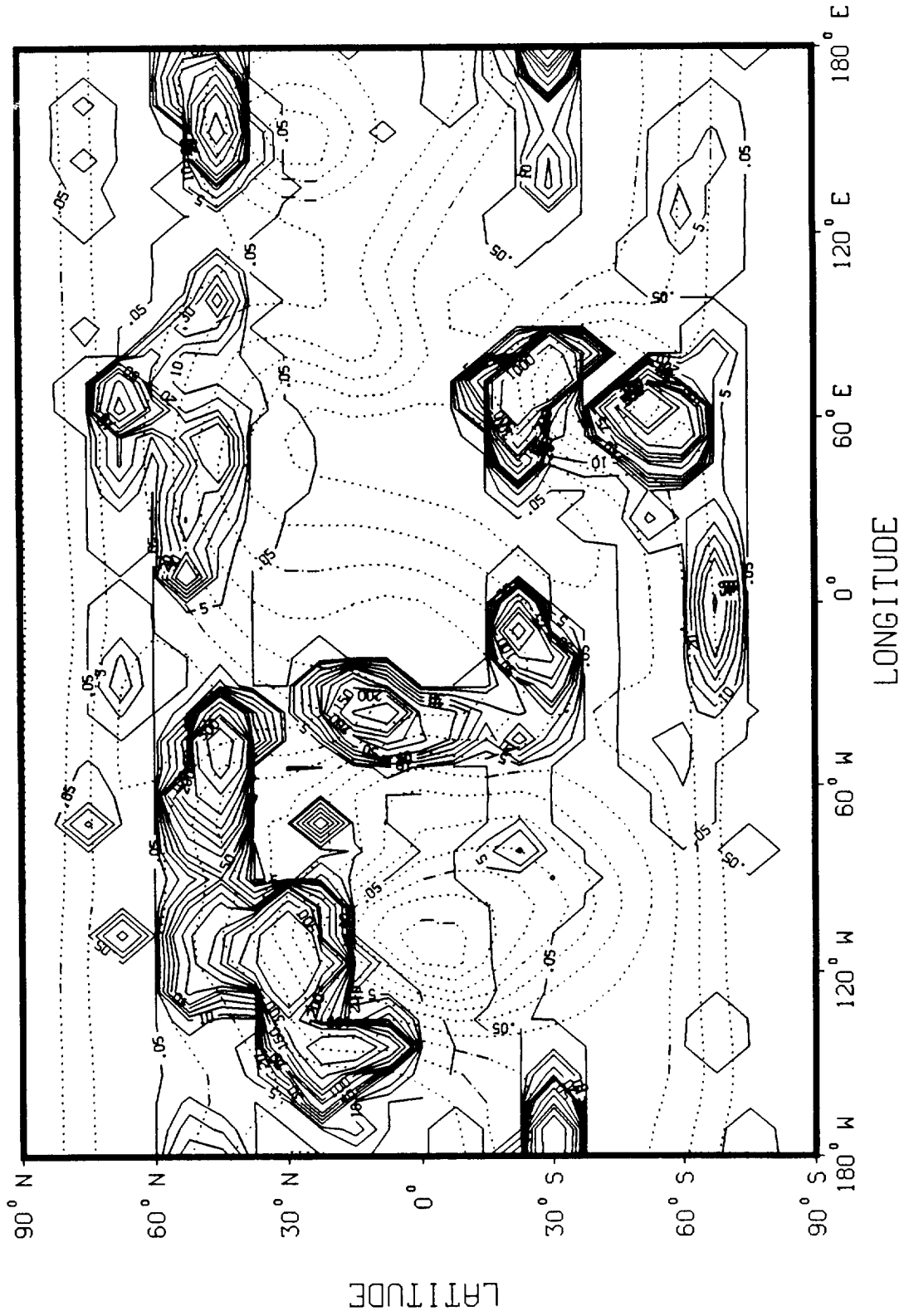


Figure 4. Map of total dust mass (grams per square meter) lifted during the initial year of the nominal simulation. Solid contours show mass lifted, dashed contours surface topography (km).

# ZONALLY AVERAGED DUST LIFTING, ( $\text{gm m}^{-2} \text{sol}^{-1}$ )

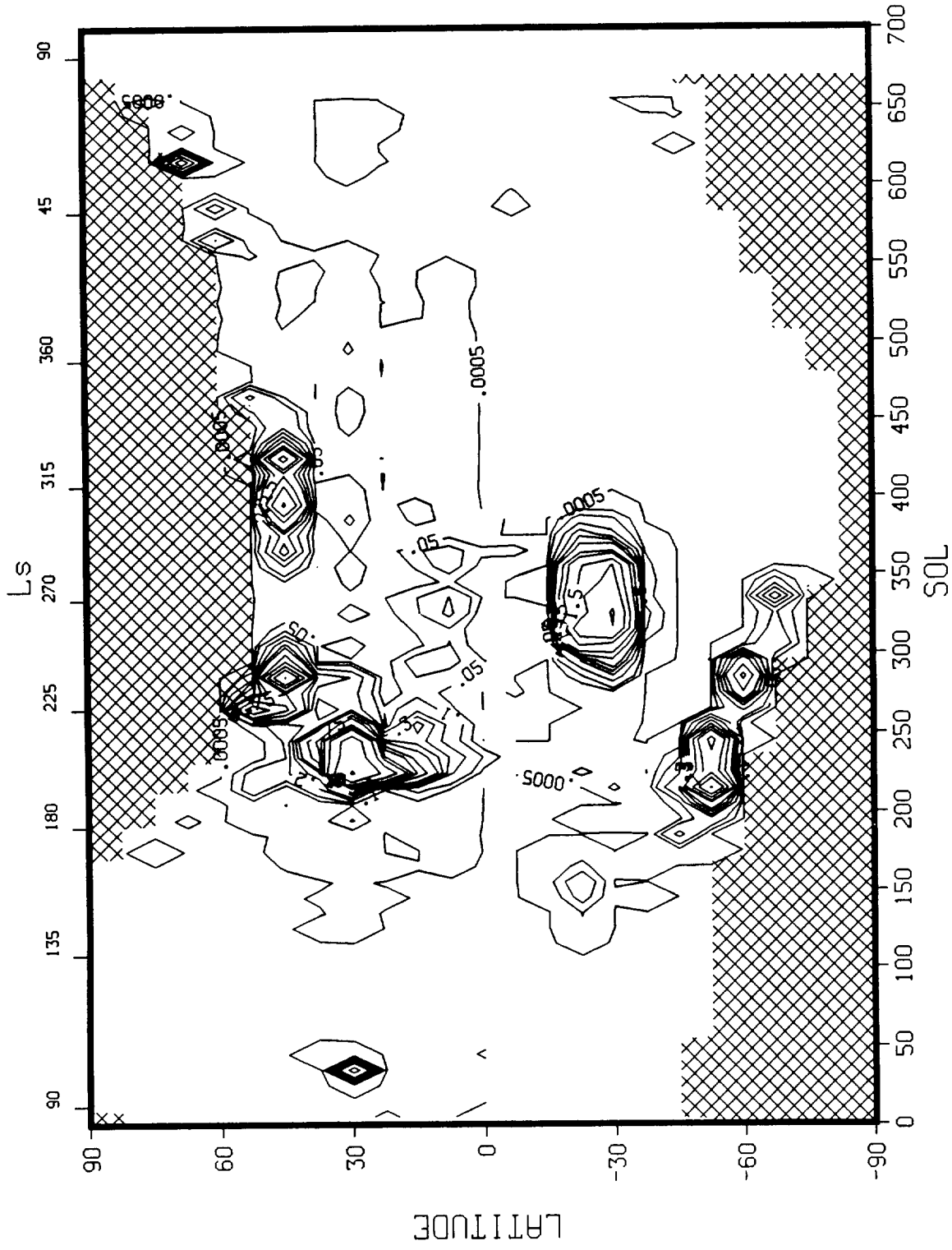


Figure 5. Time history of zonally integrated dust lifting (grams per square meters) during the course of the first year of the nominal simulation. Hatched regions correspond to the extent of the seasonal CO<sub>2</sub> ice cap, above which dust lifting is not permitted to occur.

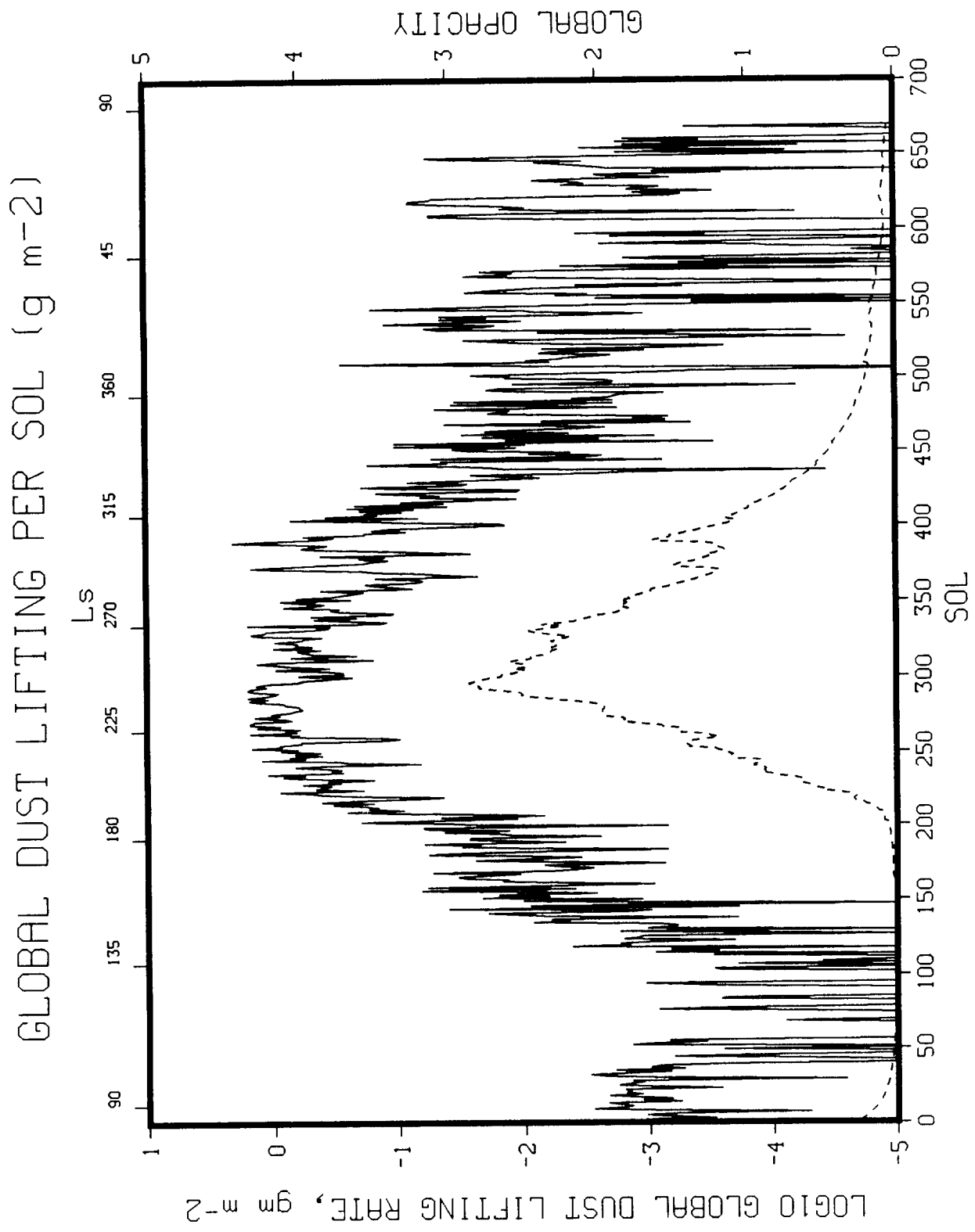


Figure 6. Time history of sol mean dust lifting rate (SOLID) and globally integrated dust optical depth (DASHED) during the course of the annual simulation in which lifted dust was radiatively inert.